JOURNAL OF COMPUTATIONAL AND THEORETICAL TRANSPORT
2023, VOL. 52, NO. 6, 429–451
https://doi.org/10.1080/23324309.2023.2287008

Comparison between Van Genuchten and Brooks-Corey Parameterizations in the Solution of Multiphase Problems in Rigid One-Dimensional Porous Media

P. H. S. Slompo[a], M. A. V. Pinto[a], and M. L. Oliveira[b]

[a]Department of Mechanical Engineering, Federal University of Paraná - UFPR, Paraná, Brazil; [b]Graduate Program in Numerical Methods in Engineering, Federal University of Paraná - UFPR, Paraná, Brazil

ABSTRACT

Multiphase problems in porous media involve the complex flow of multiple fluid phases within porous structures, covering areas of Engineering, Medicine, Geology, among others. Understanding these phenomena is crucial in natural processes, resource management, and Engineering system design. Due to its great importance, several researchers have contributed by developing different formulations to describe the multiphase problem. Through laboratory experiments, research lines emerged to numerically determine relative permeability and capillary pressure, parameters that were previously obtained only through experiments, giving rise to two distinct models to solve the flow problem: the van Genuchten and Brooks-Corey parameterizations. This work aims to analyze, through numerical simulations, the resolution of multiphase problems in rigid porous media using both parameterization models, in order to compare the efficiency of each method in different settings. Apparently, this study is unique in its focus, uncovering valuable insights into performance and applicability of both parameterization, providing a comprehensive view of their advantages and constraints in several settings. The results of this study have indicated an advantage in employing Brooks-Corey parameterization, particularly in reducing the error between the numerical and analytical solutions. The findings of this study can help, for example, to better understand oil recovery from naturally fractured reservoirs.

KEYWORDS

Two-phase flow; porous media; multigrid; modified Picard; coupled Gauss-Seidel

1. Introduction

The modeling of problems involving fluid flow in a porous structure is done by adaptations to the mass conservation law, which states that the change in mass (over time) in a given infinitesimal control volume is equal to the variation in the mass flow of fluid that passes through the control

CONTACT P. H. S. Slompo paulo.slompo@ufpr.br Department of Mechanical Engineering, Federal University of Paraná - UFPR, Paraná, Brazil.

Nomenclature

Abbreviations

BC	Brooks-Corey
VG	van Genuchten

Alphabetic Letters

C_u	Coefficient of uniformity
F_α	Source term of phase α
$\mathbf{g}$	Gravitational acceleration vector
h	Space between the grid control volumes
$itme_L$	Average of linearization iterations
$itme_{MG}$	Average of Multigrid cycle iterations
$\mathbf{K}$	Absolute permeability
$k_{r\alpha}$	Relative permeability of phase α
L	Spatial domain length
m, n	van Genuchten parameters
N	Number of samples of $time_{CPU}$
N_t	Number of time steps
N_x	Number of spatial discretization volumes
p	Fluid pressure
$\bar{p}$	Average pressures
p_c	Capillary pressure
p_e	Entry pressure
$\mathbf{q}$	Volumetric flow vector
$\|\| \cdot \|\|_\infty$	Infinity norm
res^{it}	it-th residual iteration
res^0	Initial estimate residual
$C.V.$	Coefficient of variation
S	Saturation
$\bar{S}$	Effective saturation
$S_{\alpha r}$	Residual saturation of phase α
$timeCPU$	CPU time
T	Final time
TOL	Multigrid method tolerance

Greek Letters

∇	Gradient operator
δp	Pressure correction
γ	Arithmetic mean of *time*CPU
λ	Brooks-Corey parameter
λ_α	Fluid mobility of phase α
μ	Fluid viscosity
Ω	Continuous domain
Ω^h	Fine grid
Ω^{2h}	Coarse grid
ρ	Fluid density
ϕ	Porosity of the medium
τ	Time interval

Subscripts

α	Fluid phase
*bc*0	Boundary condition at x 0
*bc*L	Boundary condition at x L
n	Non-wet phase of the fluid
w	Wet phase of the fluid

Superscripts

n	Time step iteration
m	Linearization method iteration

volume together with the contribution of sources and sinks within this same volume (Bastian 1999).

Applying this law to two immiscible fluids, wetting (w) and non-wetting (n), both flowing through the same porous medium, we obtain the mathematical model of interest. This model consists of a highly nonlinear system of partial differential equations, making its resolution by common analytical or iterative methods difficult, with one possible solution being the use of suitable numerical methods. To solve these equations, it is necessary to perform spatial and temporal discretization, as well as linearization.

In the literature, there are numerous discretization models for partial differential equations. For spatial discretization, there are various methods such as the finite difference method (LeVeque 2007), finite volume method (Versteeg and Malalasekera 2007), and finite element method (Hughes 2000), among others. For temporal discretization, Euler, Crank-Nicolson, and Runge-Kutta methods (Ferziger and Peric 2002) are widely used. In this work, we chose to use the Finite Volume Method and Implicit Euler for spatial and temporal discretization, respectively.

Given the nonlinearity of the model in question, we apply a linearization method to the nonlinear system in order to approximate it to a system of linear equations. Some examples of linearization methods are Newton's and Picard's method (Ferziger and Peric 2002; Burden and Faires 2016). In our analysis, we use a method derived from Picard's method, the Modified Picard (Celia and Binning 1992).

With the use of these discretization and linearization methods, linear systems are generated that need to be solved at each linearization step (Burden and Faires 2016). Such systems can be solved using direct or iterative methods. The chosen discretization and linearization methods for this problem generate large sparse matrices, often making the use of direct methods impractical for their resolution. In the specific case of this work, which deals with a simplified one-dimensional problem, the generated matrices are tridiagonal, and they can be easily solved using the Tridiagonal Matrix Algorithm (TDMA) (Burden and Faires 2016). However, in order to generalize our study, we have chosen to use only iterative methods. The main methods for solving linear problems are the Jacobi and the Gauss-Seidel methods (Burden and Faires 2016). However, these iterative methods lose the ability to reduce the full spectrum of errors as the number of iterations increases. The Multigrid method (Trottenberg, Oosterlee, and Schuller 2001; Oliveira, Franco, and Pinto 2018; De Oliveira et al. 2018; Malacarne, Pinto, and Franco 2022) is a numerical technique used to solve this type of problem. This method uses a hierarchy of grids to cover the entire spectrum of errors and thus accelerate convergence.

The use and development of multipahse flow in porous media simulations can be applied in supervision, study, control, and the development of new techniques, such as deep-sea oil extraction, as the soil filled with this fossil fuel can be considered a porous medium (Wang et al. 2020). Similarly, we can apply this model to study soil contaminated by toxic waste, such as pesticides and liquids from improper waste disposal (Brewer, Dror, and Berkowitz 2022), monitor tumor growth in patients, and even control and seek more effective and less aggressive methods in chemotherapy treatment for oncology (Mascheroni, Santagiuliana, and Schrefler 2019).

A real application on multiphase flow in porous media can be discussed in Chamkha (2000a). That study considers flow of two immiscible fluids

viscous, incompressible, and electrically heat-conducting in an impermeable channel filled with a uniform porous medium. That study is useful in understanding the effects of thermal buoyancy and a magnetic field on enhanced oil recovery and filtration systems.

Applications in multiphase flow and heat transfer in a horizontal channel and free-convective flow of micropolar and viscous fluids in a vertical channel can be seen in Umavathi et al. (2005) and Kumar et al. (2010).

The problem of flow and heat transfer in an electrically conducting fluid or the hydromagnetic natural convection heat transfer using a two-phase model in porous media, both in the presence of a magnetic field, are studied in Chamkha (2000b) and Khanafer and Chamkha (1998).

In Chamkha (2002) and Chamkha and Al-Naser (2001) can be found double-diffusive convection in the cases where is analyzed a porous enclosure with cooperating temperature gradient and heat generation/absorption effects, or an inclined porous enclosure with opposing temperature gradient, both with concentration gradients.

A research line of interest in multiphase flow is the search for parameterizations, that is, the search for analytical relationships to determine variables so that it is no longer necessary to define them through laboratory experiments. Two of these parameterizations seek to model the relationships between fluid saturation and the variables of capillary pressure and relative permeability, namely the well-known parameterizations of van Genuchten (van Genuchten 1980) and Brooks-Corey (Brooks and Corey 1964).

An important application of the van Genuchten (VG) and Brooks-Corey (BC) models can be discussed in Dejam and Hassanzadeh (2011). That work develops a mechanistic model for the formation of liquid bridges that cause interaction between blocks in fractured porous media, thus advancing the understanding of two-phase flows in this type of media.

This work aims to analyze the effectiveness of each of these parameterizations in solving one-dimensional multiphase problems in rigid porous media. Through numerical analysis, we will compare various parameters, such as the infinity norm of the errors of the variables of interest (pressure and saturation), average number of linearizations, average number of iterations in the multigrid method, and number of iterations in the coupled Gauss-Seidel solver. A representation of this problem is illustrated in Figure 1, where two phases, such as water and oil, flow through a one-dimensional rigid porous medium.

This study distinguishes itself from existing references by focusing on the comparative analysis of two distinct parameterization methods, whereas most literature primarily emphasizes parameter estimation (Yang and You 2013; Han, Shao, and Horton 2010; Wang, Horton, and Shao 2002) and applications (Liang et al. 2016; Akhmetov, Kuleshova, and Mukhametshin

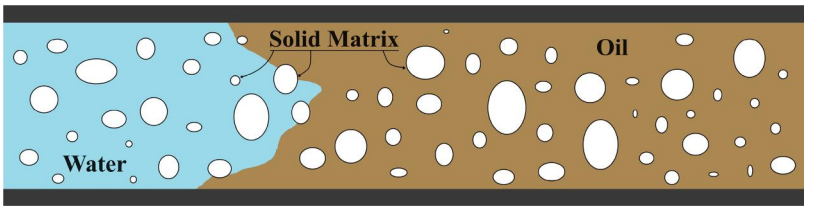

Figure 1. Illustration of a one-dimensional porous medium filled with two fluids, water and oil.

2019) of these methods, but rarely incorporates both parameterizations in their research. Works that do consider both methods typically focus only on finding parameters that approximate the parameterization models rather than directly comparing them (Lenhard, Parker, and Mishra 1989; Benson et al. 2014; Pan et al. 2019). In our work, we propose a method that that calculates the approximation between the relative permeabilities by measuring the difference between the areas under these curves.

There are also studies that make such comparisons (Abbaspour et al. 2012; Goorabjiri and Rasoulzadeh 2016; Pan et al. 2019), but they are often more focused on the aspect of fluid flow in soils, which makes them more specific than the present work. Those studies often involve experimental soil analysis to determine specific parameters tailored to the problem they aim to solve. In contrast, our study places a stronger emphasis on the theoretical and mathematical aspects, striving to achieve the best numerical model performance without considering specific cases and physical parameters.

Furthermore, our research introduces a new perspective by incorporating the multigrid method to aid in the convergence of the numerical model. The inclusion of the multigrid method enhances the robustness and efficiency of our numerical model, setting our work apart from others in the same domain.

One significant advantage of this study is that it proposes an equation that relates the parameters of VG and BC. Another notable advantage is the ease of extending the problem to two dimensions, because the parameters of VG and BC are independent of them.

However, there are also some limitations to the study. One drawback is that transitioning to a three-phase scenario might not be as immediate due to the inherent complexity involved. Another limitation is that the capillary pressure expressions were not included in the numerical models and were replaced by a single expression proposed by Illiano (2016).

The rest of this article is organized as follows: Section 2 develops the mathematical and numerical model underlying the problem; Section 3 presents the equations of the analyzed parameterizations; Section 4 introduces the Multigrid method; Section 5 demonstrates the results of the simulations, and finally, in Section 6 we present the conclusions.

2. Mathematical and numerical models

Flow in rigid porous media, for two immiscible fluids, follows the model of the mass conservation differential equation for each phase α (Bastian 1999)

$$\frac{\partial(\rho_\alpha \theta_\alpha)}{\partial t} + \nabla \cdot (\rho_\alpha \mathbf{q}_\alpha) = F_\alpha, in\ \ \Omega \times \tau, \tag{1}$$

where $\alpha = w, n$ with w representing the wetting phase and n the non-wetting phase, ρ_α is the fluid density, $\theta_\alpha = \phi S_\alpha$ where ϕ is the porosity of the medium and S_α is the saturation, $\mathbf{q}_\alpha$ is the volumetric flow rate, F_α is the source term corresponding to phase α, and $\nabla \cdot$ is the divergence operator. Since we are dealing with a one-dimensional problem, the domain of the flow differential equation is $\Omega = \mathbb{R}^+$ and τ is a given time interval $(0, T]$, where T is the final time. The volumetric flow rate is given by Darcy's law adapted for multiphase flow (Bastian 1999)

$$\mathbf{q}_\alpha = -\lambda_\alpha \mathbf{K}(\nabla p_\alpha - \rho_\alpha \mathbf{g}), \tag{2}$$

where $\lambda_\alpha = \frac{k_{r\alpha}}{\mu_\alpha}$ is the mobility, with $k_{r\alpha}(S_\alpha)$ being the relative permeability (dimensionless value), μ_α is the dynamic viscosity of the fluid, $\mathbf{K}$ is the absolute permeability, which depends only on the porous medium, p_α is the pressure of phase α fluid, $\mathbf{g}$ is the acceleration due to gravity vector, and ∇ is the gradient operator.

Remark 1. Darcy's law is valid for the slow flow, therefore, convective effects can be neglected (Bastian 1999).

By substituting Equation (2) into Equation (1), considering incompressible fluids and zero gravity acceleration, we obtain the equation for the problem, given by the pressure-saturation formulation (Illiano 2016):

$$\frac{\partial \theta_\alpha}{\partial t} - \nabla \cdot (\lambda_\alpha \mathbf{K} \nabla p_\alpha) = \frac{F_\alpha}{\rho_\alpha}. \tag{3}$$

In multiphase flow problems, the interaction between different phases gives rise to a pressure at the interface between the fluids, called capillary pressure:

$$p_c = p_n - p_w. \tag{4}$$

To complete the mathematical formulation of the problem, we use Dirichlet boundary conditions given by $p_\alpha(0, t) = p_{\alpha \mathrm{bc0}}$ and $p_\alpha(L, t) = p_{\alpha \mathrm{bcL}}$, where $p_{\alpha \mathrm{bc0}}$ and $p_{\alpha \mathrm{bcL}}$ are the known boundary conditions, and L is the length of the spatial domain.

Remark 2. It can be noted that this work assumes thermal equilibrium of the multiphase with the porous medium. This case appears in real situations. In Smaï (2023), the main assumptions of the formulation for multiphase compositional flows are: the solid matrix is inert and non deformable and the porous system is always at thermal local equilibrium. Thermodynamic

equilibrium is also assumed in Coatleven and Meiller (2021), which deals with applications in real cases.

Remark 3. It can also be noted that the non-Darcian inertia effects have been neglected. But there are cases where these effects must be considered. For more details, see Chamkha (1996, 1997), where continuous and volume-mean equations governing the non-Darcy hydromagnetic free and mixed convection flows are developed.

In order to obtain the numerical model, we discretize Equation (3) with respect to time using the implicit Euler method with $\Delta t = \frac{T}{N_T}$, where N_T is the number of time steps. We then use the modified Picard method to linearize the resulting equations. For simplicity, we use the notations $C_\alpha = \frac{\partial \theta_\alpha}{\partial p_c}$ and $K_\alpha = \mathbf{K}\frac{k_{r\alpha}}{\mu_\alpha}$. This process is performed for both phases w and n, resulting in the following equations:

$$C_w^{n+1,m}\frac{\delta p_n^{n+1,m+1} - \delta p_w^{n+1,m+1}}{\Delta t} - \frac{\partial}{\partial x}\left[K_w^{n+1,m}\frac{\partial}{\partial x}(\delta p_w^{n+1,m+1})\right] = \frac{\partial}{\partial x}\left[K_w^{n+1,m}\frac{\partial}{\partial x}(p_w^{n+1,m})\right] + F_w^{n+1} - \frac{\theta_w^{n+1,m} - \theta_w^n}{\Delta t}, \tag{5a}$$

$$-C_w^{n+1,m}\frac{\delta p_n^{n+1,m+1} - \delta p_w^{n+1,m+1}}{\Delta t} - \frac{\partial}{\partial x}\left[K_n^{n+1,m}\frac{\partial}{\partial x}(\delta p_n^{n+1,m+1})\right] = \frac{\partial}{\partial x}\left[K_n^{n+1,m}\frac{\partial}{\partial x}(p_n^{n+1,m})\right] + F_n^{n+1} - \frac{\theta_n^{n+1,m} - \theta_n^n}{\Delta t}, \tag{5b}$$

where $\delta p_\alpha^{n+1,m+1} = p_\alpha^{n+1,m+1} - p_\alpha^{n+1,m}$ is the pressure correction for phase α. In Equations (5a, 5b) the superscripts $n+1$ and $m+1$ represent the current time level and the current iteration of linearization, respectively.

Additionally, we use the Finite Volume Method with a uniform mesh for the spatial discretization of Equations (5a, 5b). In this process, we use the Gauss divergence theorem (Kreyszig 2011) and calculate the resulting integrals using the matrix form of the volume locations. By using nodal values to calculate the approximations at the faces for pressures and their corrections, we obtain the following linear expression:

$$[C_w]_j^{n+1,m}\left([\delta p_n]_j^{n+1,m+1} - [\delta p_w]_j^{n+1,m+1}\right)\frac{\Delta x}{\Delta t} - \left\{[K_w]_{j+\frac{1}{2}}^{n+1,m}\left(\frac{[\delta p_w]_{j+1}^{n+1,m+1} - [\delta p_w]_j^{n+1,m+1}}{\Delta x}\right) - [K_w]_{j-\frac{1}{2}}^{n+1,m}\left(\frac{[\delta p_w]_j^{n+1,m+1} - [\delta p_w]_{j-1}^{n+1,m+1}}{\Delta x}\right)\right\}\frac{1}{\mu_w} = \left\{[K_w]_{j+\frac{1}{2}}^{n+1,m}\left(\frac{[p_w]_{j+1}^{n+1,m+1} - [p_w]_j^{n+1,m+1}}{\Delta x}\right) - [K_w]_{j-\frac{1}{2}}^{n+1,m}\left(\frac{[p_w]_j^{n+1,m+1} - [p_w]_{j-1}^{n+1,m+1}}{\Delta x}\right)\right\}\frac{1}{\mu_w} + \left[\frac{[F_w]_j^{n+1,m}}{\rho_w} - \frac{[\theta_w]_j^{n+1,m} - [\theta_w]_j^n}{\Delta t}\right]\Delta x, \tag{6}$$

where $\Delta x = \frac{L}{N_x}$ is the distance between the centers of the volumes in the discretized domain, L is the length of the domain Ω and N_x is the number of volumes.

Rearranging Equation (6) to solve for the correction of the wetting pressure δp_w and repeating the entire process for the correction of the non-wetting pressure δp_n, we obtain the following linear system that must be solved at each linearization step (De Oliveira et al. 2020),

$$\begin{bmatrix} A_w & B \\ B & A_n \end{bmatrix} \begin{bmatrix} \delta p_w \\ \delta p_n \end{bmatrix} = \begin{bmatrix} f_w \\ f_n \end{bmatrix}, \tag{7}$$

where,

$$A_\alpha = \begin{bmatrix} bc & 0 & & & & & & \\ [a_\alpha]_{i-1} & [a_\alpha]_i & [a_\alpha]_{i+1} & 0 & & & & \\ 0 & [a_\alpha]_{i-1} & [a_\alpha]_i & [a_\alpha]_{i+1} & 0 & & & \\ & \ddots & \ddots & \ddots & \ddots & & & \\ & & & 0 & [a_\alpha]_{i-1} & [a_\alpha]_i & [a_\alpha]_{i+1} & \\ & & & & & 0 & bc & \end{bmatrix},$$

$$B = \begin{bmatrix} bc & 0 & & & & & \\ 0 & c_i & 0 & & & & \\ & 0 & c_i & 0 & & & \\ & & \ddots & \ddots & \ddots & & \\ & & & & 0 & c_i & 0 \\ & & & & & 0 & bc \end{bmatrix},$$

with

$$[a_\alpha]_i = -\left[C_w^{n+1,m}\right]_i + \frac{\Delta t}{\Delta x^2}\left(\left[K_\alpha^{n+1,m}\right]_{i-\frac{1}{2}} + \left[K_\alpha^{n+1,m}\right]_{i+\frac{1}{2}}\right),$$

$$[a_\alpha]_{i+1} = -\frac{\Delta t}{\Delta x^2}\left[K_\alpha^{n+1,m}\right]_{i+\frac{1}{2}},$$

$$[a_\alpha]_{i-1} = -\frac{\Delta t}{\Delta x^2}\left[K_\alpha^{n+1,m}\right]_{i-\frac{1}{2}},$$

$$c_i = \left[C_w^{n+1,m}\right]_i,$$

$$[f_\alpha]_i = \frac{\Delta t}{\Delta x^2}\left[K_\alpha^{n+1,m}\right]_{i+\frac{1}{2}}\left[p_\alpha^{n+1,m}\right]_{i+1} - \frac{\Delta t}{\Delta x^2}\left(\left[K_\alpha^{n+1,m}\right]_{i-\frac{1}{2}} + \left[K_\alpha^{n+1,m}\right]_{i+\frac{1}{2}}\right)\left[p_\alpha^{n+1,m}\right]_i + \frac{\Delta t}{\Delta x^2}\left[K_\alpha^{n+1,m}\right]_{i-\frac{1}{2}}\left[p_\alpha^{n+1,m}\right]_{i-1} + \Delta t F_\alpha - \left[\theta_\alpha^{n+1,m}\right]_i + \left[\theta_\alpha^n\right]_i.$$

3. Parameterizations

Capillary pressure and relative permeabilities are parameters usually determined through laboratory experiments. In this section, we will discuss two methods found in the literature to determine these parameters: van Genuchten (VG) and Brooks-Corey (BC) parameterizations.

3.1. Van Genuchten parameterization

In the van Genuchten (VG) parameterization, capillary pressure and relative permeabilities of the w and n phases can be expressed as follows (Bastian 1999):

$$p_c(S_\alpha) = p_e\left(\bar{S}_\alpha^{\frac{-1}{m}} - 1\right)^{\frac{1}{n}}, \tag{8}$$

$$k_{rw}(S_w) = \sqrt{\bar{S}_w}\left(1 - \left(1 - \bar{S}_w^{\frac{1}{m}}\right)^m\right)^2, \tag{9}$$

$$k_{rn}(S_w) = \sqrt{1 - \bar{S}_w}\left(1 - \bar{S}_w^{\frac{1}{m}}\right)^{2m}, \tag{10}$$

where p_e and n are free parameters of VG, $\bar{S}_\alpha$ is the effective saturation of phase α, and $m = 1 - \frac{1}{n}$. The parameter p_e is called the entry pressure and represents the critical pressure required for the non-wetting phase to enter the larger pores of the medium (Bastian 1999). The parameter n is physically related to the symmetry in the distribution of pore sizes. According to Lenhard, Parker, and Mishra (1989) and Benson et al. (2014), n takes on low values when the medium has a highly asymmetric pore size distribution, and high values for a more uniform distribution.

The relationship between the free parameter n and the physical properties of the medium was explored by Benson et al. (2014) through empirical tests using the coefficient of uniformity (C_u), which is a physical parameter indicating the degree of pore size uniformity in the medium. In this case, a large C_u refers to an asymmetric medium, and as C_u tends to 1, the pores tend to have a constant size. The Figure 2 (adapted from (Benson et al. 2014)) illustrates the relationship between C_u and the free parameter n. It can be observed that for media with low asymmetry (small C_u values close to 1), the typical values of n can vary significantly, mainly concentrating in the range between 2 and 8. On the other hand, for highly asymmetric media (high C_u), the values of this parameter remain close to 2. Therefore, it can be concluded that when there is high asymmetry, an approximation can be made by taking the value of n as 2, unlike the opposite case (high degree of symmetry) where there is no strict criterion for the choice of n.

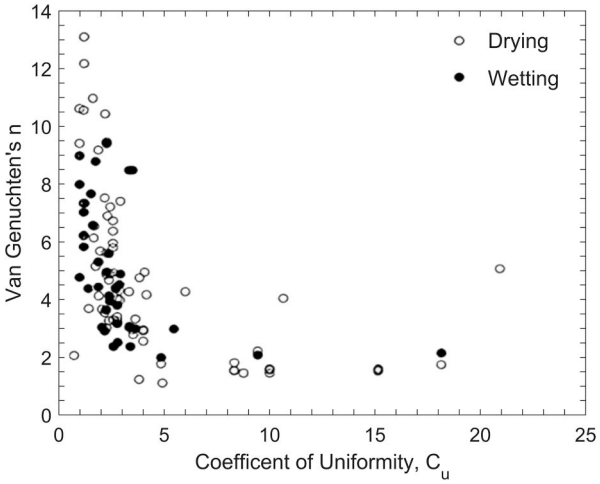

Figure 2. *n versus* C_u adapted from Benson et al. (2014).

Finally, $\bar{S}_\alpha$ represents the effective saturation of phase α and can be described as:

$$\bar{S}_w = \frac{S_w - S_{wr}}{1 - (S_{wr} - S_{nr})}, \tag{11}$$

where $S_{\alpha r}$ is the residual saturation of phase α ($\alpha = w$ and n).

3.2. Brooks-corey parameterization

For the model developed by Brooks and Corey (1964) (BC), the capillary pressure and relative permeabilities of the w and n phases can be obtained through the following equations:

$$p_c(S_\alpha) = p_e \bar{S}_\alpha^{\frac{-1}{\lambda}}, \tag{12}$$

$$k_{rw}(S_w) = \bar{S}_w^{\frac{2+3\lambda}{\lambda}}, \tag{13}$$

$$k_{rn}(S_w) = (1 - \bar{S}_w)^2 \left(1 - \bar{S}_w^{\frac{2+\lambda}{\lambda}}\right), \tag{14}$$

where p_e and λ are the free parameters. Similarly to the VG model, p_e represents the entry pressure. The parameter λ is physically related to the distribution of pore sizes: the more uniform the porous medium, the higher the value of λ. The opposite occurs for non-uniform media.

According to Bastian (1999), typical values for λ range from 0.2 to 3. Corey (1994) suggests typical values of λ around 2. In natural sandbanks, this value concentrates between 5 and 6, especially if the material is well-mixed and compacted. For untouched soils (highly asymmetric), values of λ below 1 are not uncommon (Corey 1994).

4. Solver and multigrid method

After temporal discretization, linearization, and spatial discretization using the MVF of the studied model, as shown in Section 2, large sparse systems arise, such as those given by Equation (7), in each step of linearization of the two-phase problem equation system. Such systems can be solved using direct or iterative methods (referred to as solvers here). Nevertheless, the direct method is not efficient for solving this type of system (Barrett et al. 1994; Burden and Faires 2016), so we prioritize the results generated using solvers, particularly the Gauss-Seidel coupled method (Gaspar et al. 2004).

Despite the method rapidly reducing the high-frequency components of the error (oscillatory modes), it encounters difficulties in reducing the low-frequency components (smooth modes). This results in a rapid decay of the error in the early iterations of the process, but as the iterations progress, the reduction rate starts to decrease, and the error begins to decrease slowly, eventually stabilizing. To overcome this situation, we use the Multigrid method, which is a robust method designed to accelerate the convergence of the solver by efficiently eliminating the smooth components of the error. During the problem resolution, this method goes through a hierarchy of grids with different levels of refinement, so that the smoothed errors in a fine grid are transferred to coarser grids where they gradually become more oscillatory, and convergence becomes more efficient.

For this method, two transfer operators between grids are necessary: the restriction operator, which transfers information from a fine grid (Ω^h) to the immediately coarser grid (Ω^{2h}); and the prolongation operator, which transfers information from the coarser grid to the immediately finer grid. In this work, we use the arithmetic mean of volumes as the restriction operator and piecewise constant interpolation as the prolongation operator (Trottenberg, Oosterlee, and Schuller 2001).

During the execution of the Multigrid method, grids can be gone through in various ways, which gives rise to Multigrid cycles, the main ones being the V-, W-, F-cycles (details in Trottenberg, Oosterlee, and Schuller (2001); Wesseling (1992)). Figure 3 illustrates the W-cycle, the Multigrid cycle used in our study.

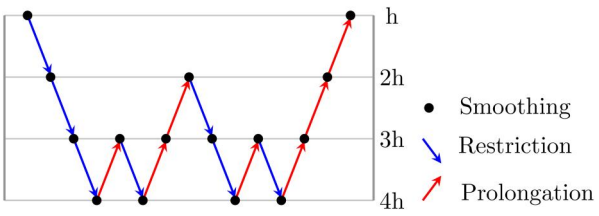

Figure 3. W-cycle for four mesh levels.

The linear system (Equation 7) originated from the discretization by the Modified Picard method (Algorithm 2) is then solved using the multigrid method (Algorithm 1).

Algorithm 1: MG-W-Cicle (l)

if $l = L_{\max}$ (coarsest grid level) **then**
  Solve $A^{(l)}v^{(l)} = f^{(l)}$ in coarse grid $\Omega^{2^{l-1}h}$.
else
  Smooth ν_1 times $A^{(l)}v^{(l)} = f^{(l)}$ on grid $\Omega^{2^{l-1}h}$ with initial guess $v_o^{(l)}$.
  Calculate and restrict the residual: $f^{(l+1)} = I_{2^{l-1}h}^{2^l h}(f^{(l)} - A^{(l)}v^{(l)})$.
  for *cicle* $= 1:2$ **do**
    Solve in the next level: **MG-W-cicle** $(l+1)$.
  end for
  Correct using prolongation: $v^{(l)} \leftarrow v^{(l)} + I_{2^l h_1 h}^{2^{l-1}h} v^{(l+1)}$.
  Smooth ν_2 times $A^{(l)}v^{(l)} = f^{(l)}$ on mesh $\Omega^{2^l h_1 h}$ with initial guess $v^{(l)}$.
end if

Where I_h^H and I_H^h are, respectively, the generic restriction and prolongation operators.

Algorithm 2: Modified Picard for two-phase problems in rigid porous media

Enter the data and initial and boundary conditions.
for $n = 1 : N_T$
  Update θ_α.
  while *not reaching the stopping criterion for the linearization step* **do**
    Calculate C_w, $k_{r\alpha}$ and F_α.
    Update θ_α.
    while *not reaching the stopping criterion for the Multigrid* **do**
      One Multigrid cycle in the system (7) using **MG-W-cicle(1)**.
    end while
  end while
end for

5. Results

5.1. Numerical experiments

The algorithms used in this work were implemented in MATLAB R2016a with double precision on a device equipped with an AMD Ryzen 5-5500 U 2.1 GHz processor, 8GB of RAM, and the Windows 11 64-bit operating system.

In order to verify the implemented codes, we compared the obtained numerical solutions with the analytical solution of the problem proposed by Illiano (2016), which has simple data, facilitating the calculations

involved. The analytical expressions for the saturation of the wetting phase w (S_w) and the average of the pressures ($\bar{p} = \frac{p_w + p_n}{2}$) are given by $S_w(x,t) = \bar{p}(x,t) = xt(1-x)$, with initial and boundary conditions given by $f(x,0) = f(0,t) = f(1,t) = 0$. Additionally, Illiano (2016) also proposes an analytical expression for the capillary pressure; which in practice means that we will not use the parameterization for this variable. This expression is given by $p_c(S_w) = 1 - \frac{1}{2}{S_w}^2$.

For the pressure-saturation formulation (given by Equation 3), our approach involves solving the linearized systems in the variables δp_w and δp_n (pressure corrections) (according to Equation (7)). Some modifications were necessary for Illiano (2016) problem to fit our simulations and enable the use of p_w and p_n instead of $\bar{p}$. Using Equation (4) we obtain the following expressions:

$$p_w = \bar{p} - \frac{p_c}{2} \text{ and } p_n = \bar{p} + \frac{p_c}{2}.$$

In order to obtain an analytical model that relates the VG and BC parameterizations, we used comparable free parameters from each of them, namely n for VG and λ for BC. These parameters were employed to ensure that the curves of the relative permeabilities (k_{rw} and k_{rn}) approximate each other.

There are already analytical expressions in the literature that relate n and λ as a function $\lambda = g(n)$ (Lenhard, Parker, and Mishra 1989; Benson et al. 2014; Pan et al. 2019). In this work, we propose the choice of these parameters based on the calculation of the total area between the curves of the relative permeabilities (k_{rw} and k_{rn}). This method will be referred to as the Area Difference method. It involves calculating the area between the curves of the relative permeabilities. This area, denoted as

$$A(n,\lambda) = \int_0^1 [|k_{rwVG} - k_{rwBC}| + |k_{rnVG} - k_{rnBC}|] dS_w, \tag{15}$$

where $A(n,\lambda)$ represents the area between the curves, $k_{r\alpha P}$ denotes the relative permeability of phase α (where $\alpha = w$ or n), P denotes the parameterization method (P = VG or BC), and S_w represents the saturation of the wetting phase. The objective of this method is to find a λ value, given an n value, that minimizes the area between the curves of the relative permeabilities (with n for VG and λ for BC). This calculation can be expressed as

$$\min_{\lambda} A(n,\lambda), \text{ for a given } n. \tag{16}$$

To test the effectiveness of the expressions found in the literature and the Area Difference method, we calculated the corresponding λ values for certain specific n values (see Table 1). In this case, the last column

Table 1. λ values corresponding to certain n values for four different methods.

n	(Lenhard, Parker, and Mishra 1989) $\lambda = (n-1)(1-0.5^{\frac{n}{n-1}})$	(Benson et al. 2014) $\lambda = 0.05 + 0.39n$	(Pan et al. 2019) $\lambda = 0.451n - 0.263$	Area Difference λ from Equation (16)	Area –
2	0.75	0.83	0.64	0.28	2.078
3	1.29	1.22	1.09	0.72	1.321
4	1.81	1.61	1.54	1.20	1.000
5	2.32	2.00	1.99	1.71	0.847
6	2.82	2.39	2.44	2.25	0.768
7	3.33	2.78	2.89	2.79	0.726
8	3.83	3.17	3.35	3.31	0.702

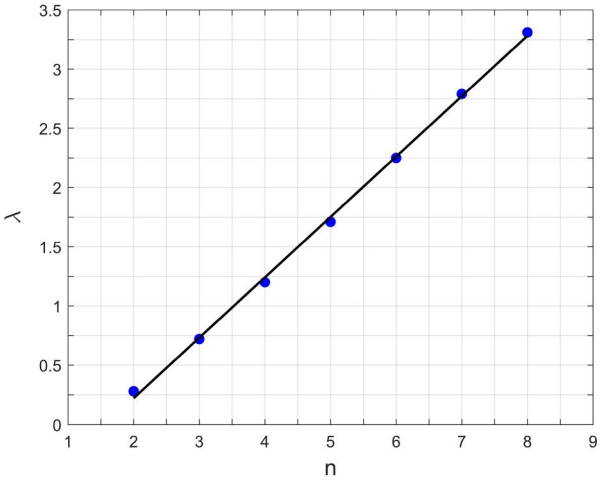

Figure 4. Linear fit between λ and n for the Area Difference method.

represents the minimum area achieved with the specified n value and the λ value shown in the column related to the Area Difference method.

Despite the differences in the results obtained between the functions defined by Lenhard, Parker, and Mishra (1989), Benson et al. (2014) and Pan et al. (2019) and the Area Difference method proposed in this work, a similar behavior can be observed, especially with the expressions of Benson et al. (2014) and Pan et al. (2019).

Figure 4 shows the remarkable linear relationship between λ and n for the proposed method (column" Area Difference" in Table 1). By performing a linear fit (Devore 2012; Burden and Faires 2016), we obtain the following relationship

$$\lambda(n) = 0.51n - 0.7986. \tag{17}$$

The derived expression establishes a relationship between the free parameters of each parameterization, resulting in the smallest area between the curves of the relative permeabilities. However, it is important to note that even though this relationship exists, it does not guarantee that the resulting areas will always have values small enough to be considered comparable

parameters. An illustrative example of this is when $n = 2$ and $\lambda = 0.28$ which yields an area between curves of 0.2078. This value is relatively high compared to the areas obtained with larger n. Nevertheless, it is crucial not to disregard comparisons using the free parameter from VG. As discussed in Section 3.1, $n = 2$ provides the best approximation for media with highly asymmetric pore sizes, which is a realistic setting.

Establishing this new correspondence model between VG and BC parameters, validated through a comparison with the Lenhard, Parker, and Mishra (1989), Benson et al. (2014) and Pan et al. (2019) models and built upon a robust method, which is the Area Difference method, we can confirm that this procedure is correct and will be employed throughout the rest of the study.

Taking this into consideration, we used a few integer values for n, adjusted the value of λ using the proposed expression (Equation (17)) and selected three pairs of parameters for our comparisons (see Table 2). The value $n = 2$ was considered because it represents a realistic situation of highly asymmetric pores. The other values ($n = 4$ and 5) were selected because they have relatively low area between the curves of the relative permeabilities of the two phases (see Table 1 and Figure 5) and because they are typical parameters (see Figure 2). The parameters for Test 4, in addition to having a small area between the curves (Figure 5), also have a typical λ (see Section 3.2).

The plots of the curves of the relative permeabilities of the two phases for the chosen parameters are shown in Figure 5.

In our simulations, we used a porosity of $\phi = 0.9$ (highly porous physical medium), densities and viscosities of each phase as $\rho_w = \rho_n = \mu_w = \mu_n = 1$. Additionally, in order to simplify the calculations, we disregarded the residual saturations, i.e., $S_{\alpha r} = 0$ ($\alpha = w$ and n).

The simulations performed using the data from Test 1 in Table 2 generated the graphs in Figures 6 and 7, respectively, for the VG and BC parameterizations, comparing the analytical and numerical solutions of the saturation of the wetting phase (S_w) at certain time steps and mesh sizes. It is possible to observe that in all cases we have excellent numerical approximations for both parameterizations.

Therefore, a code verification was performed using the analytical solution proposed by Illiano (2016), confirming the validity of both models.

Table 2. Free parameters n and λ used in the numerical simulations.

	n	λ
Test 1	5.00	1.75
Test 2	4.00	1.24
Test 3	2.00	0.22
Test 4	5.48	2.00

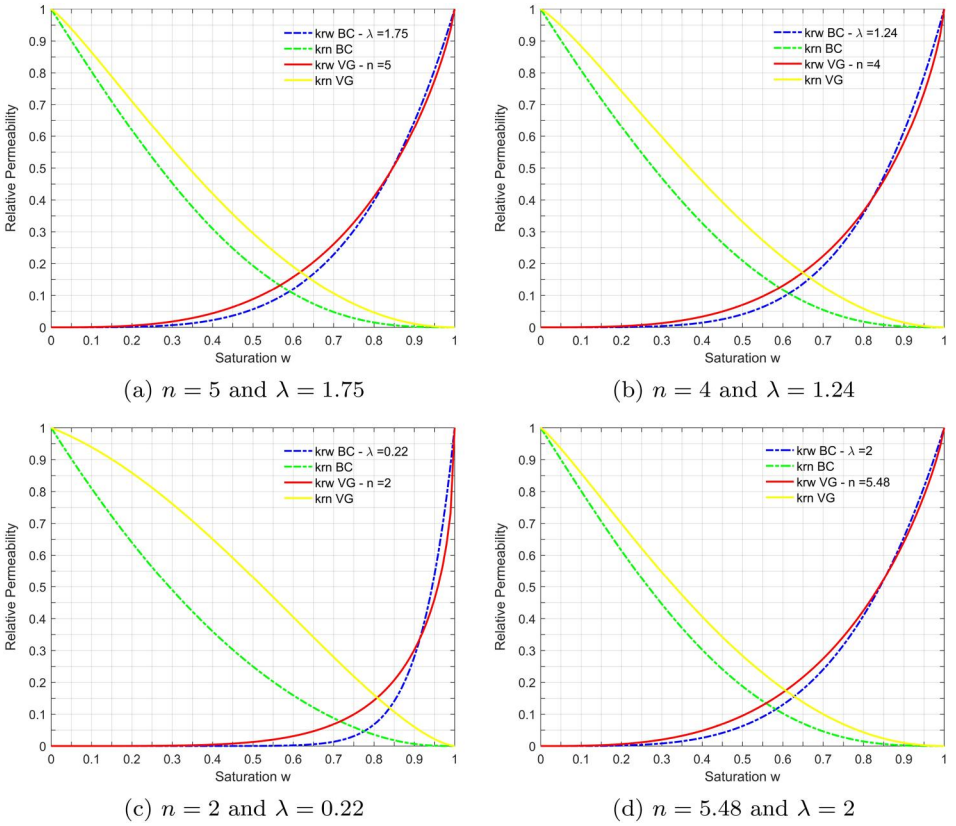

(a) $n = 5$ and $\lambda = 1.75$ (b) $n = 4$ and $\lambda = 1.24$

(c) $n = 2$ and $\lambda = 0.22$ (d) $n = 5.48$ and $\lambda = 2$

Figure 5. Curves of the relative permeabilities of the wetting and non-wetting phases for various n and λ parameters for VG and BC parameterizations.

5.2. Results analysis

In order to facilitate comparisons between the VG and BC parameterizations, we conducted multiple simulations using different values for the free parameters of each method, as outlined in Table 2. All the results discussed in this section were obtained utilizing the Multigrid method. The stopping criterion for the iterative process was determined based on the infinity norm of the dimensionless residual,

$$\frac{||res^{it}||_\infty}{||res^0||_\infty} \leq TOL,$$

where res^{it} is the residual of a given iteration, res^0 is the residual in the initial estimate, and TOL is the tolerance, adopted as 10^{-5}. For the linearization process, the stopping criterion used was the maximum, in absolute value, of the corrections to the pressures of the wetting and non-wetting phases, δp_w and δp_n, with a tolerance of 10^{-8}.

Table 3 presents the main data obtained in the simulations of Tests 1 to 4 for the VG and BC parameterizations, where $itme_L$ is the average of

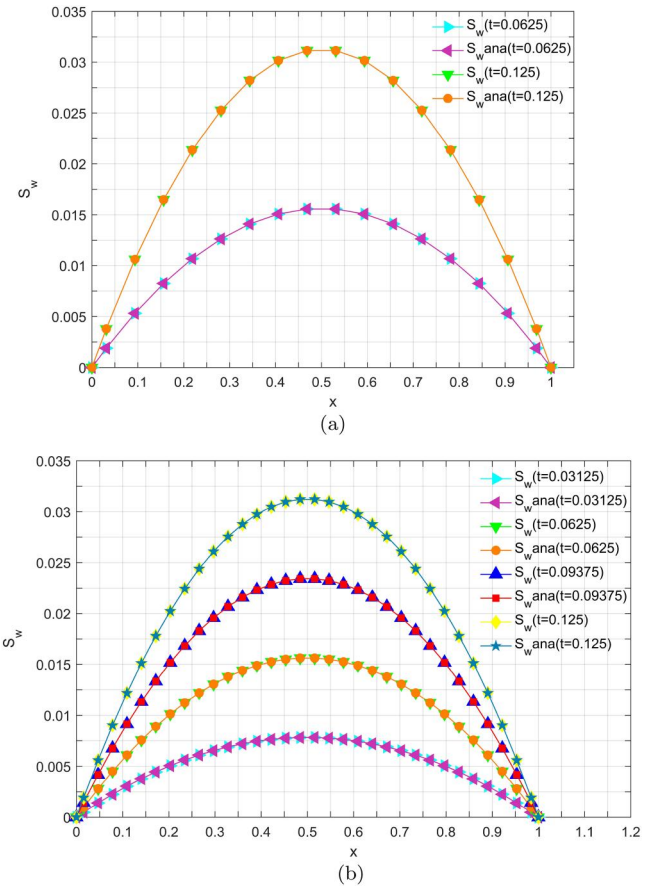

Figure 6. Numerical and analytical solutions for S_w using the VG parameterization with $n = 5$ at different time steps for a mesh (a) $N_x = N_t = 16$ and (b) $N_x = N_t = 32$.

linearization iterations, $itme_{MG}$ is the average of Multigrid cycle iterations, and γ is the program execution time. In the column γ_{VG}/γ_{BC}, values greater than 1 indicate that VG had the longest execution time, and values smaller than 1 indicate the opposite.

Since the Matlab $time_{CPU}$ function is sensitive to short times, γ was calculated as the arithmetic mean of a certain number of samples N, where N was defined based on the standard deviation (s) and the coefficient of variation (C.V.) (Santos and Dias 2021)).

According to Costa (2015) a C.V. value $\leq$15% indicates a distribution with low dispersion, implying homogeneity in the analyzed data. Thus, for selecting suitable sample sizes, we only considered samples with C.V. $<$15%. Consequently, the majority of simulations presented in Table 3 exhibited an average computational time γ with C.V. $<$5%.

Analyzing Table 3 we can observe that the obtained values of $itme_L$ and $itme_{MG}$ for both methods are low and very similar, confirming the

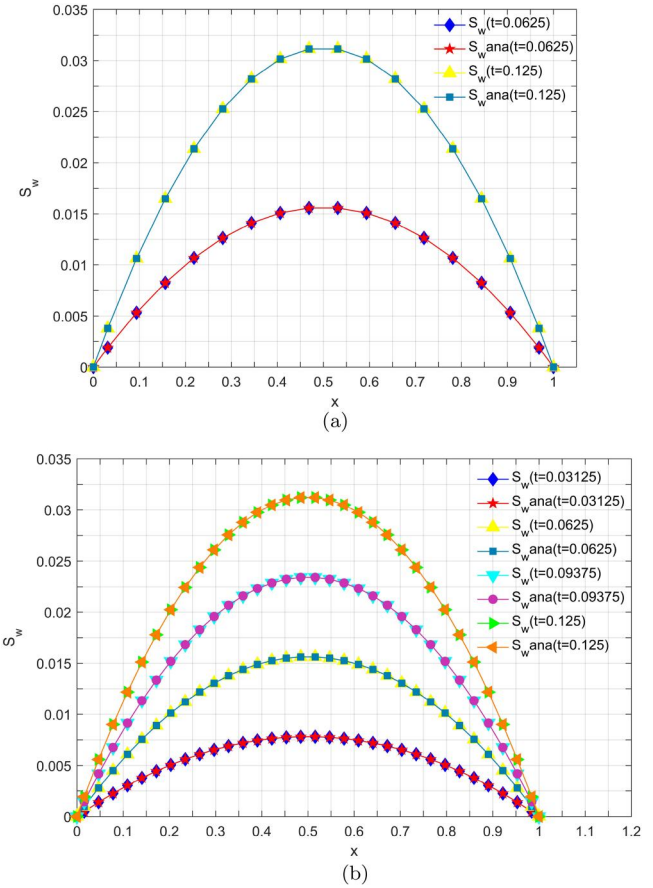

Figure 7. Numerical and analytical solutions for S_w using the BC parameterization with $\lambda = 1.75$ at different time steps for a mesh (a) $N_x = N_t = 16$ and (b) $N_x = N_t = 32$.

robustness and efficiency of both parameterizations. Based on the execution times (γ) of both methods and the ratio γ_{VG}/γ_{BC} between them, we noticed a slight advantage of the BC parameterization over the VG parameterization, with $\gamma_{VG}/\gamma_{BC} > 1$ in tests 1 and 2, and a slight advantage of VG, with $\gamma_{VG}/\gamma_{BC} < 1$, in tests 3 and 4. Since the values are very close, a new criterion is needed to determine which parameterization is more suitable. Considering this situation, we will analyze the decrease in error as the number of variables increases.

Figure 8 shows the infinity norm of the errors for p_w and p_n for the parameters of the four settings presented in Table 2. In this case, the infinity norm of the error is shown as a function of the variation of $N_x = N_t$. The results obtained demonstrate that the BC parameterization tends to reduce the errors more efficiently for values of the VG free parameter n different from 2. However, when $n = 2$, both parameterizations have similar capabilities in reducing such errors.

Table 3. $itme_L$, it_{MG}, γ and γ_{VG}/γ_{BC} for different VG and BC parameters and mesh sizes.

		VG			BC			
Test	$N_x = N_t$	$itme_L$	it_{MG}	γ	$itme_L$	$itme_{MG}$	γ	γ_{VG}/γ_{BC}
	8	6.50	2	0.25	6.00	2	0.23	1.0870
	16	5.50	3	1.25	5.31	3	1.28	0.9766
1	32	5.09	3	6.13	5.13	3	5.91	1.0372
	64	4.48	3	24.92	4.30	3	23.41	1.0645
	128	4.06	3	107.63	4.07	3	106.99	1.0060
	8	6.13	2	0.26	5.88	2	0.23	1.1304
	16	5.38	3	1.45	5.31	3	1.32	1.0985
2	32	5.09	3	5.92	5.13	3	6.11	0.9689
	64	4.38	3	24.79	4.27	3	24.47	1.0131
	128	4.05	3	108.06	4.07	3	109.43	0.9875
	8	5.63	2.4	0.24	5.75	2	0.22	1.0909
	16	5.25	3	1.41	5.31	3	1.28	1.1016
3	32	4.59	3	5.34	5.00	3	6.21	0.8599
	64	4.16	3	23.16	4.25	3	23.57	0.9826
	128	4.04	3	106.13	4.07	3	107.06	0.9913
	8	6.50	2	0.38	6.13	2	0.36	1.0556
	16	5.50	3	1.50	5.31	3	1.65	0.9091
4	32	5.09	3	6.15	5.13	3	6.30	0.9762
	64	4.55	3	25.58	4.34	3	25.41	1.0067
	128	4.06	3	108.55	4.07	3	114.93	0.9445

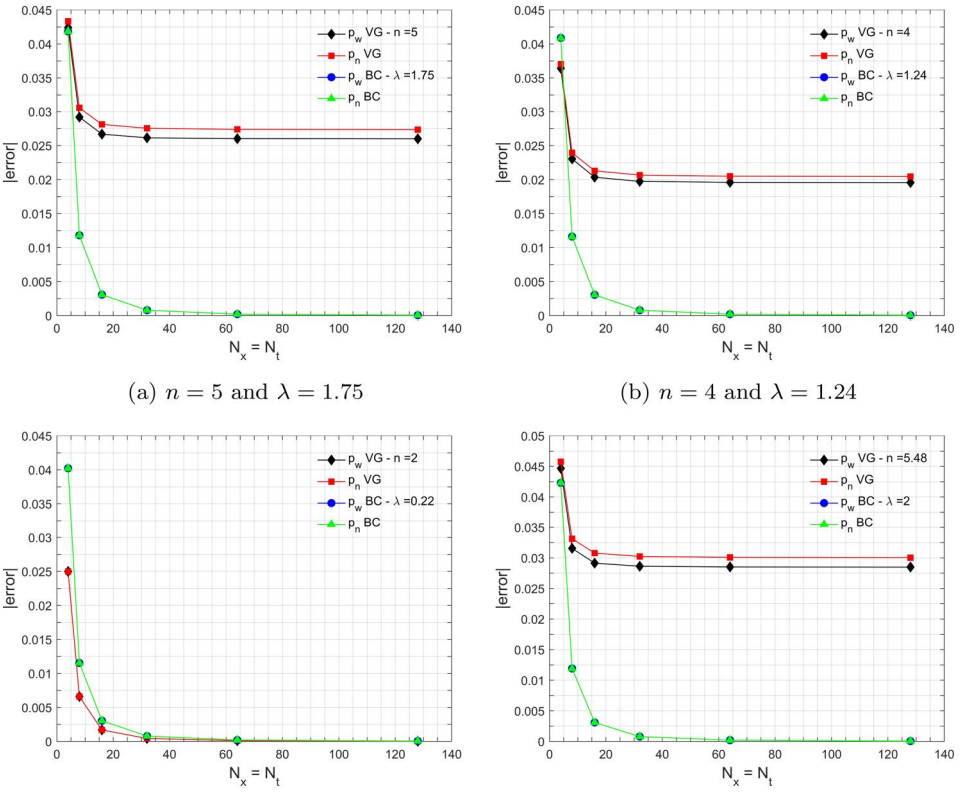

(a) $n = 5$ and $\lambda = 1.75$

(b) $n = 4$ and $\lambda = 1.24$

(c) $n = 2$ and $\lambda = 0.22$

(d) $n = 5.48$ and $\lambda = 2$

Figure 8. Infinity norm of errors for some VG and BC parameters.

6. Summary and conclusions

In this study, we compared the two main parameterizations found in the literature for solving multiphase flow problems in rigid porous media: van Genuchten and Brooks-Corey. Throughout the work, we presented the expressions that compose each parameterization method, and the relationships between mathematical and physical parameters. We verified our code by comparing the numerical solution with the analytical one.

1. The results obtained in the simulations demonstrated that both parameterizations are robust and have similar average iterations for both linearization and Multigrid.
2. Regarding the decrease in the infinity norm of numerical errors, the Brooks-Corey parameterization has a significant advantage when the analyzed media has more uniform pore sizes ($n \neq 2$).
3. In a highly asymmetric porous media ($n = 2$), both parameterizations reduce the infinity norm of the error similarly, with the Brooks-Corey parameterization having a slight advantage due to lower CPU time.

Acknowledgments

The authors would acknowledge the Fundação da Universidade Federal do Paraná - Brazil (FUNPAR) and the infrastructure provided by the Department of Mechanical Engineering (DEMEC) of Federal University of Paraná (UFPR).

Disclosure statement

The authors hereby confirm that they are the sole liable persons responsible for the authorship of this work, and that all material that has been herein included as part of the present paper is either the property (and authorship) of the authors.

Funding

This study was financed by the Fundação da Universidade Federal do Paraná - Brazil (FUNPAR).

References

Abbaspour, H., M. Shorafa, R. Daneshfaraz, M. H. Mohammadi, and M. Rashtbari. 2012. Study and comparison the efficiency of mualem-van genuchten and brooks-corey models in predicting unsaturated hydraulic conductivity in compacted soils. *J. Civil Eng. Urban.* 2 (2):56–62.

Akhmetov, R., L. Kuleshova, and V. Mukhametshin. 2019. Application of the Brooks-Corey model in the conditions of lower cretaceous deposits in terrigenous reservoirs of Western Siberia. 560:07. IOP Conference Series: Materials Science and Engineering.

Barrett, R., M. Berry, T. F. Chan, J. Demmel, J. Donato, J. Dongarra, V. Eijkhout, R. Pozo, C. Romine, and H. van der Vorst. 1994. Templates for the solution of linear systems: Building blocks for iterative methods. 2nd ed. Philadelphia: Society for Industrial and Applied Mathematics.

Bastian, P. 1999. Numerical computation of multiphase flows in porous media. Master's thesis, University of Kiel, Kiel.

Benson, C., I. Chiang, T. Chalermyanont, and A. Sawangsuriya. 2014. Estimating van genuchten parameters α and n for clean sands from particle size distribution data. 02. 410–427. doi:10.1061/9780784413265.033

Brewer, A., I. Dror, and B. Berkowitz. 2022. Electronic waste as a source of rare earth element pollution: Leaching, transport in porous media, and the effects of nanoparticles. *Chemosphere* 287 (Pt 2):132217. doi:10.1016/j.chemosphere.2021.132217.

Brooks, R. H., and A. T. Corey. 1964. Hydraulic properties of porous media. *Hydrol. Paper* (3): 21–5.

Burden, R. L., and J. D. Faires. 2016. *Numerical analysis*. 10th ed. Boston: Cengage Learning.

Celia, M. A., and P. Binning. 1992. A mass conservative numerical solution for two-phase flow in porous media with application to unsaturated flow. *Water Resour. Res.* 28 (10): 2819–28. doi:10.1029/92WR01488.

Chamkha, A. J. 1996. Non-Darcy hydromagnetic free convection from a cone and a wedge in porous media. *Int. Commun. Heat Mass Transfer.* 23 (6):875–87. doi:10.1016/0735-1933 (96)00070-X.

Chamkha, A. J. 1997. Non-darcy fully developed mixed convection in a porous medium channel with heat generation/absorption and hydromagnetic effects. *Numer Heat Transfer Part A Appl.* 32 (6):653–75. doi:10.1080/10407789708913911.

Chamkha, A. J. 2000a. Flow of two-immiscible fluids in porous and nonporous channels. *J. Fluids Eng. Transact. Asme J. Fluid Eng.* 122 (1):117–24. doi:10.1115/1.483233.

Chamkha, A. J. 2000b. Unsteady laminar hydromagnetic fluid–particle flow and heat transfer in channels and circular pipes. *Int. J. Heat Fluid Flow* 21 (6):740–6. doi:10.1016/S0142-727X(00)00031-X.

Chamkha, A. J. 2002. Double-diffusive convection in a porous enclosure with cooperating temperature and concentration gradients and heat generation or absorption effects. *Numer Heat Transfer Part A Appl.* 41 (1):65–87. doi:10.1080/104077802317221447.

Chamkha, A. J., and H. Al-Naser. 2001. Double-diffusive convection in an inclined porous enclosure with opposing temperature and concentration gradients. *Int. J. Therm. Sci.* 40 (3):227–44. doi:10.1016/S1290-0729(00)01213-8.

Coatleven, J., and C. Meiller. 2021. On an efficient time scheme based on a new mathematical representation of thermodynamic equilibrium for multiphase compositional Darcy flows in porous media. *Comput. Geosci.* 25 (3):1063–82. doi:10.1007/s10596-021-10039-0.

Corey, A. T. 1994. *Mechanics of immiscible fluids in porous media*. Colorado: Water Resources Publications.

Costa, G. G. O. 2015. *Basic statistics course (in Portuguese)*. 2nd ed. São Paulo: Atlas.

De Oliveira, M. L., M. A. V. Pinto, C. Rodrigo, F. J. Gaspar, and S. R. Franco. 2020. L-scheme and modified Picard with multigrid method for a 1D two-phase problem in rigid porous media with analytical solution. In Proceedings of the XLI Ibero-Latin-American Congress on Computational Methods in Engineering, ABMEC, Foz Do Iguaçu/PR, Brazil.

De Oliveira, M. L., M. A. V. Pinto, S. d F. Tomazzoni, and G. V. Rutz. 2018. On the robustness of the xy-Zebra-gauss-seidel smoother on an anisotropic diffusion problem. *Cmes.* 117 (2):251–70. doi:10.31614/cmes.2018.04237.

Dejam, M., and H. Hassanzadeh. 2011. Formation of liquid bridges between porous matrix blocks. *Alche. J.* 57 (2):286–98. doi:10.1002/aic.12262.

Devore, J. L. 2012. *Probability & statistics for engineering and the sciences*. 8th ed. Boston: Cengage Learning.

Ferziger, J. H., and M. Peric. 2002. *Computational methods for fluid dynamics*. 3rd ed. New York: Springer.

Gaspar, F. J., F. J. Lisbona, C. W. Oosterlee, and R. Wienands. 2004. A systematic comparison of coupled and distributive smoothing in multigrid for the poroelasticity system. *Num. Linear Algebra App.* 11 (2–3):93–113. doi:10.1002/nla.372.

Goorabjiri, M. H., and A. Rasoulzadeh. 2016. Comparison of accuracy of van Genuchten and brooks & Corey models for simulating water flow in forest floor using HydroGeoSphere code. *J. Water Soil* 30 (3):984–96.

Han, X.-W., M.-A. Shao, and R. Horton. 2010. Estimating van Genuchten model parameters of undisturbed soils using an integral method. *Pedosphere* 20 (1):55–62. doi:10.1016/S1002-0160(09)60282-4.

Hughes, T. J. R. 2000. *The finite element method: Linear static and dynamic finite element analysis*. 1st ed. Mineola, NY: Dover Publications.

Illiano, D. 2016. Iterative schemes for solving coupled, non-linear flow and transport in porous media. Master's thesis, University of Bergen.

Khanafer, K. M., and A. J. Chamkha. 1998. Hydromagnetic Natural Convection From an Inclined Porous Square Enclosure with Heat Generation. *Num. Heat Transfer Part A Appl.* 33 (8):891–910. doi:10.1080/10407789808913972.

Kreyszig, E. 2011. *Advanced engineering mathematics*. 10th ed. Hoboken, NJ: John Wiley & sons.

Kumar, J. P., J. C. Umavathi, A. J. Chamkha, and I. Pop. 2010. Fully-developed free-convective flow of micropolar and viscous fluids in a vertical channel. *Appl. Math. Modell.* 34 (5):1175–86. doi:10.1016/j.apm.2009.08.007.

Lenhard, R., J. Parker, and S. Mishra. 1989. On the correspondence between brooks-corey and van genuchten models. *J. Irrig. Drain. Eng.* 115 (4):744–51. doi:10.1061/(ASCE)0733-9437(1989)115:4(744).

LeVeque, R. J. 2007. *Finite difference methods for ordinary and partial differential equations*. 1st ed. Philadelphia: Society for Industrial and Applied Mathematics.

Liang, X., V. Liakos, O. Wendroth, and G. Vellidis. 2016. Scheduling irrigation using an approach based on the van Genuchten model. *Agric. Water Manage.* 176:170–9. doi:10.1016/j.agwat.2016.05.030.

Malacarne, M. F., M. A. V. Pinto, and S. R. Franco. 2022. Performance of the multigrid method with timestepping to solve 1D and 2D wave equations. *Int. J. Comput. Methods Eng. Sci. Mech.* 23 (1):45–56. doi:10.1080/15502287.2021.1910750.

Mascheroni, P., R. Santagiuliana, and B. Schrefler. 2019. Multiphase porous media models for mechanics in medicine: Applications to transport oncophysics and diabetic foot. In *Encyclopedia of biomedical engineering*, edited by Roger Narayan, 155–66. Oxford: Elsevier.

Oliveira, F. d., S. R. Franco, and M. A. V. Pinto. 2018. The effect of multigrid parameters in a 3d heat diffusion equation. *Int. J. Appl. Mech. Eng.* 23 (1):213–21. doi:10.1515/ijame-2018-0012.

Pan, T., S. Hou, Y. Liu, and Q. Tan. 2019. Comparison of three models fitting the soil water retention curves in a degraded alpine meadow region. *Sci. Rep.* 9 (1):18407. doi:10.1038/s41598-019-54449-8.

Santos, C., and C. Dias. 2021. Note on the coefficient of variation properties. *Braz. Elect. J. Math.* 2 (4):101–11. doi:10.14393/BEJOM-v2-n4-2021-58062.

Smaï, F. F. 2023. A thermodynamic formulation for multiphase compositional flows in porous media. https://api.semanticscholar.org/CorpusID:263737328.

Trottenberg, U., C. Oosterlee, and A. Schuller. 2001. *Multigrid*. San Diego: Academic Press.

Umavathi, J. C., A. J. Chamkha, A. Mateen, and A. Al-Mudhaf. 2005. Unsteady two-fluid flow and heat transfer in a horizontal channel. *Heat Mass Transfer.* 42 (2):81–90. doi:10.1007/s00231-004-0565-x.

van Genuchten, M. T. 1980. A closed-form equation for predicting the hydraulic conductivity of unsaturated soils. *Soil Sci. Soc. Amer. J.* 44 (5):892–8. doi:10.2136/sssaj1980.03615995004400050002x.

Versteeg, H. K. and Malalasekera. 2007. *An introduction to computational fluid dynamics the finite volume method*. 2nd ed. London: Pearson Education.

Wang, Q., R. Horton, and M. Shao. 2002. Horizontal infiltration method for determining brooks-corey model parameters. *Soil Sci. Soc. Amer. J.* 66 (6):1733–9. doi:10.2136/sssaj2002.1733.

Wang, Y., T. Lu, H. Zhang, Y. Li, Y. Song, J. Chen, X. Fu, Z. Qi, and Q. Zhang. 2020. Factors affecting the transport of petroleum colloids in saturated porous media. *Colloids Surf, A.* 585:124134. doi:10.1016/j.colsurfa.2019.124134.

Wesseling, P. 1992. *An introduction to multigrid methods*. Chichester: John Wiley & Sons.

Yang, X., and X. You. 2013. Estimating parameters of van genuchten model for soil water retention curve by intelligent algorithms. *Appl. Math. Inf. Sci.* 7 (5):1977–83. doi:http://doi.org/10.12785/amis/070537.